Point 5: $\tilde{\chi}_1^{\pm}$ and $\tilde{\chi}_2^0$ Pair Production at the ILC

Madalina Chera

ILD Analysis/Software Phone Meeting

12.02.2014

Point 5

"Point 5" benchmark : gaugino pair production at ILC

http://arxiv.org/pdf/1006.3396.pdf (ILD LoI)

http://arxiv.org/pdf/0911.0006v1.pdf (SiD LoI)

ATLAS-CONF-2013-035

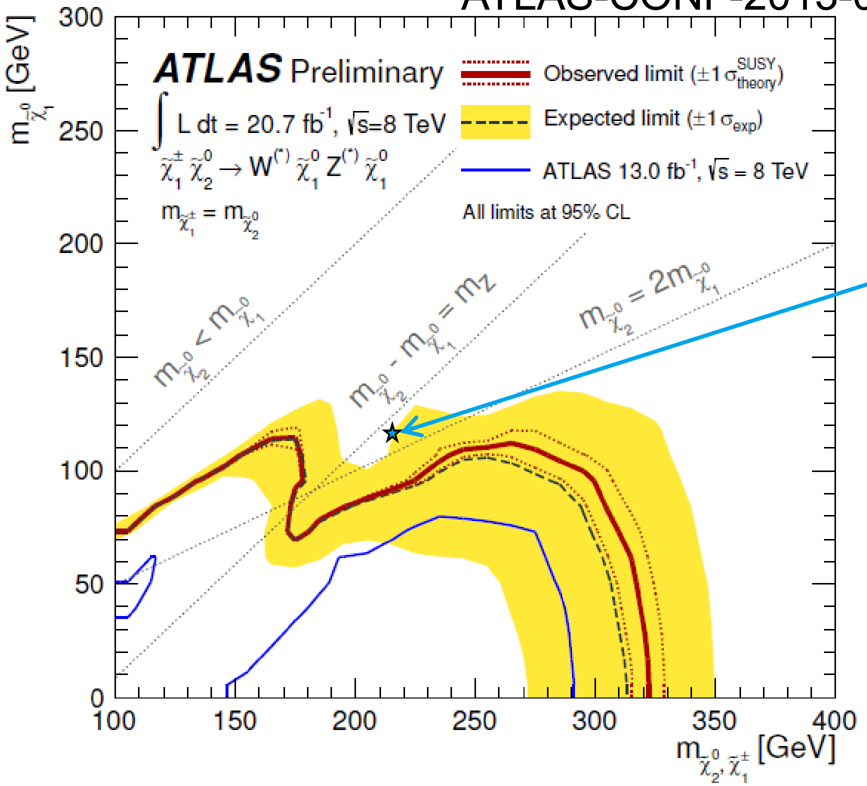

Particle	Mass [GeV]
$\tilde\chi_1^0$	115.7
$\tilde\chi_1^\pm$	216.5
$\tilde\chi_2^0$	216.7
$\tilde\chi_3^0$	380

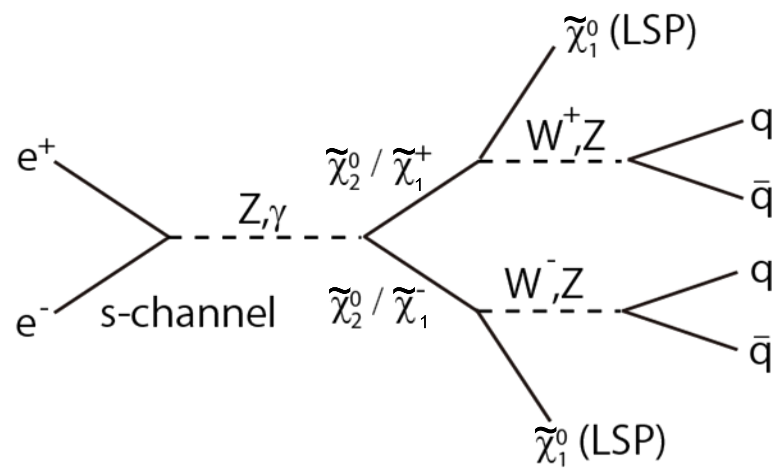

Point 5 - motivation

> The „point 5“ scenario is a good case for:

> studying the detector and particle flow performance

- 2 escaping LSP’s → missing energy
- hadronic decay of gauge bosons
- goal: clearly distinguish between W and Z pair events

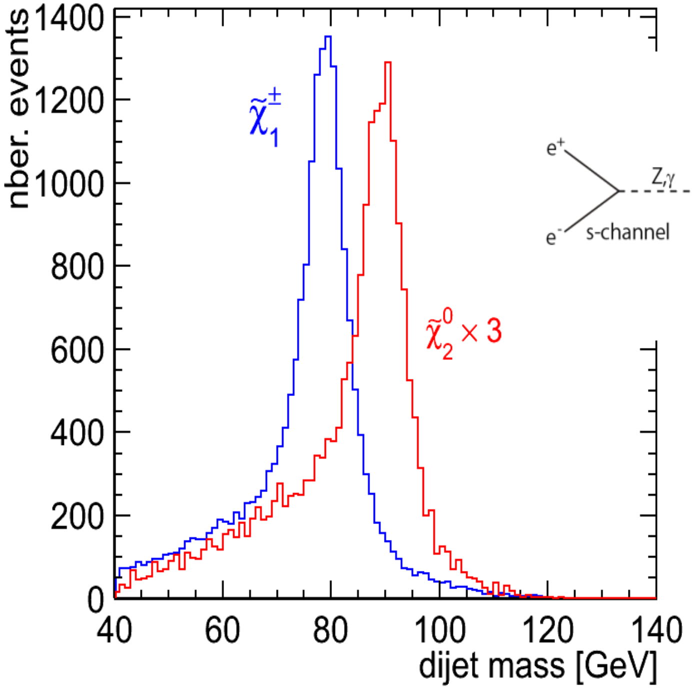

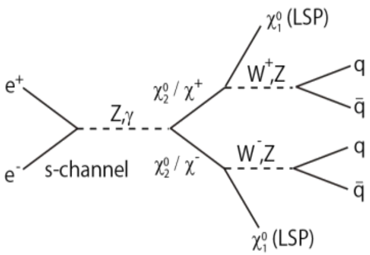

> **comparing and studying the performance of two versions of detector simulation (e.g. LOI and DBD)**

Data Samples:

> Signal: 40000 $\tilde{\chi}_1^{\pm}$ events and 9000 $\tilde{\chi}_2^0$ events

> **LOI sample:**	> **DBD sample:**
▪ Signal generated with `Whizard1.51` Background generated with `Whizard1.40` ▪ **Note:** in the signal samples, the M_W was inadvertently lowered by Whizard to M_W = 79.8 GeV	▪ Used the same **signal** generator files as in the LOI sample
▪ Signal + background were simulated and reconstructed with `ilcsoft v01-06`	▪ Re-simulated and re-reconstructed ONLY the **signal** samples with `ilcsoft v01-16-02.` ▪ Used the existing LOI SM samples for background
▪ The jet energy scale was increased by 1%	▪ The jet energy scale was not increased for the DBD produced signal
▪ No $\gamma\gamma$ background overlay	▪ No $\gamma\gamma$ background overlay
▪ The analysis was re-run on existing data samples	▪ The analysis was re-run

Data Samples:

> Signal: 40000 $\tilde{\chi}_1^{\pm}$ events and 9000 $\tilde{\chi}_2^0$ events

> **LOI sample:**	> **DBD sample**:
▪ Signal generated with `Whizard1.51` Background generated with `Whizard1.40` ▪ **Note:** in the signal samples, the M_W was inadvertently lowered by Whizard to M_W = 79.8 GeV	▪ Used the same **signal** generator files as in the LOI sample
▪ Signal + background were simulated and reconstructed with `ilcsoft v01-06`	▪ Re-simulated and re-reconstructed ONLY the **signal** samples with `ilcsoft v01-16-02.` ▪ Used the existing LOI SM samples for background
▪ The jet energy scale was increased by 1% ▪ No $\gamma\gamma$ background overlay ▪ The analysis was re-run on existing data samples	▪ The jet energy scale was not increased for the DBD produced signal ▪ No $\gamma\gamma$ background overlay ▪ The analysis was re-run

Data Samples:

> Signal: 40000 $\tilde{\chi}_1^{\pm}$ events and 9000 $\tilde{\chi}_2^0$ events

> LOI sample:	> DBD sample:
▪ Signal generated with `Whizard1.51` Background generated with `Whizard1.40`	▪ Used the same **signal** generator files as in the LOI sample
▪ **Note:** in the signal samples, the M_W was inadvertently lowered by Whizard to M_W = 79.8 GeV	
▪ Signal + background were simulated and reconstructed with `ilcsoft v01-06`	▪ Re-simulated and re-reconstructed ONLY the **signal** samples with `ilcsoft v01-16-02.` ▪ Used the existing LOI SM samples for background
▪ The jet energy scale was increased by 1%	▪ The jet energy scale was **not** increased for the DBD produced signal
▪ No $\gamma\gamma$ background overlay ▪ The analysis was re-run on existing data samples	▪ No $\gamma\gamma$ background overlay ▪ The analysis was re-run

Study case – Analysis Flow

- The **fully hadronic** decay modes of the on shell gauge bosons were chosen as **signal**
- **Signal topology**: 4 jets and missing energy
- **Background**:
  - SM 4f background is dominant
  - Each signal channel acts as background to the other!
- Event **preselection** – apply cuts on:
  - Number of tracks in event and per jet
  - Minimum number of PFOs per jet = 3
  - Minimum jet energy and $|\cos(\theta)_{jet}|$
  - $|\cos(\theta)_{pmiss}| < 0.99$
  - $100\ \mathrm{GeV} < E_{visible} < 300\ \mathrm{GeV}$
  - $M_{missing} > 220\ \mathrm{GeV}$
- Perform **kinematic fit** using `MarlinKinFit`: equal mass constraint (determine best jet pairing and improve resolution)
  - Apply cut on converged kinematic fit

CUT	$\tilde{\chi}_1^{\pm}$ had	$\tilde{\chi}_2^0$ had	Other SUSY	SMgg	SM 6f	SM 4f	SM 2f	SM Other
No cut	28548	5488	74611	2.81e+09	519242	1.3e+07	8.8e+08	4.78e+06
	28529	5488	74650	3.663e+06	521610	1.48e+07	2.14e+07	4.75e+06
Total # tracks >20	27914	5449	24318	3.03e+06	493257	6.7e+06	5.3e+06	0
	27897	5449	24305	3.03+06	495605	6.7e+06	5.3e+06	0
100 < Evis < 300 GeV	27912	5449	22518	1.05e+06	44435	949380	1.56e+06	0
	27895	5449	22508	1.06e+06	44394	959805	1.56e+06	0
Ejet > 5GeV	27906	5446	20727	908393	44137	905894	1.47e+06	0
	27889	5446	20721	908492	44096	916507	1.47e+06	0
$\lvert\cos(\theta)_{jets}\rvert < 0.99$	26572	5240	19205	350316	41130	668947	875094	0
	26560	5240	19200	350364	41098	678083	874907	0
$Y_{34} > 0.001$	26432	5218	15255	202462	38760	413787	166296	0
	26416	5218	15255	202510	38638	423080	166305	0
# tracks > 2/jet	25731	5146	9559	162161	22752	247160	145269	0
	25717	5146	9559	162193	22740	255870	145270	0
$\lvert\cos(\theta)_{miss}\rvert < 0.99$	25476	5099	9487	25097	22322	185679	4039	0
	25463	5099	9487	25087	22311	193706	4039	0
$E_l < 25$ GeV	25135	4981	6463	23129	14409	146984	3533	0
	25123	4981	6463	23133	14407	154927	3534	0
$N_{PFO} > 3$	25041	4975	6102	23014	13697	139365	3518	0
	25029	4975	6103	23014	13696	139429	3518	0
$\lvert\cos(\theta)_{Pmiss}\rvert < 0.8$	20148	4079	5179	681	9951	62676	529	0
	20144	4079	5180	681	9950	62688	529	0
Mmiss > 220 GeV	20143	4079	5179	630	3687	45875	386	0
	20139	4079	5180	630	3687	45867	389	0

Dijet [Boson] Mass Comparison – LOI to DBD

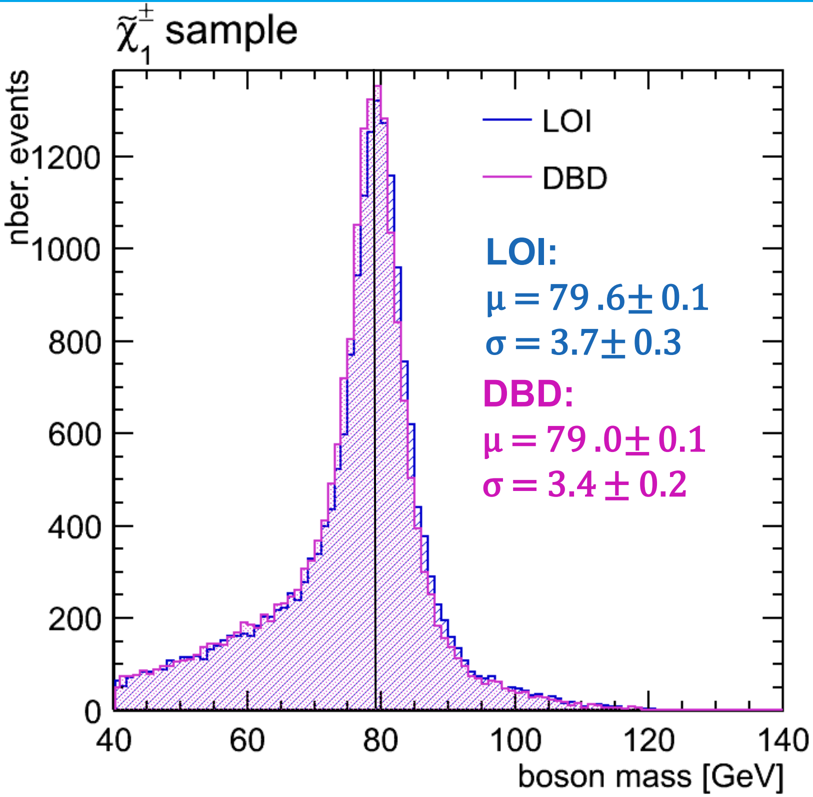

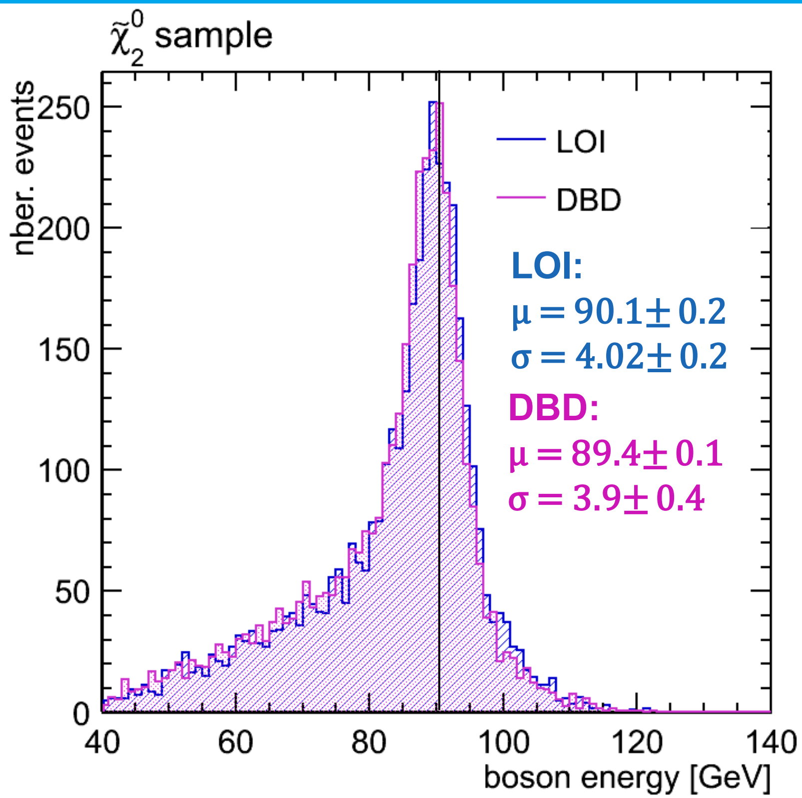

- The DBD and LOI distributions are similar.
- Compatible σ, DBD distribution slightly narrower.
- The LOI sample has a jet energy increase of 1% while the DBD sample does not.
- The DBD μ is shifted significantly to lower energies.

$\tilde{\chi}_1^{\pm}$ and $\tilde{\chi}_2^0$ Cross Section Measurement

> **Use dijet mass to separate $\tilde{\chi}_1^{\pm}$ and $\tilde{\chi}_2^0$ events → measure cross section**

> After selection cuts + kinematic fit:

Obs.	DBD		LOI	
	$\tilde{\chi}_1^{\pm}$	$\tilde{\chi}_2^0$	$\tilde{\chi}_1^{\pm}$	$\tilde{\chi}_2^0$
Efficiency	58%	64%	57%	65%
Purity	57%	12%	57%	13%

Example: DBD sample

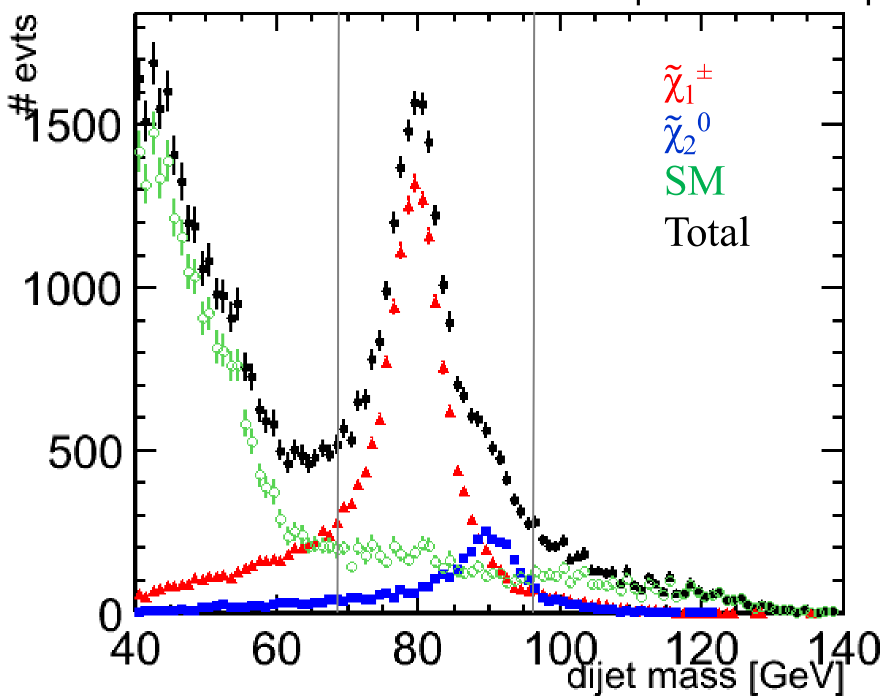

> Perform fit to disentangle chargino and neutralino candidates

$\tilde{\chi}_1^\pm$ and $\tilde{\chi}_2^0$ Cross Section Measurement

- After KinFit → fit distribution with Voigt profile where Γ = boson natural width, σ = detector resolution:

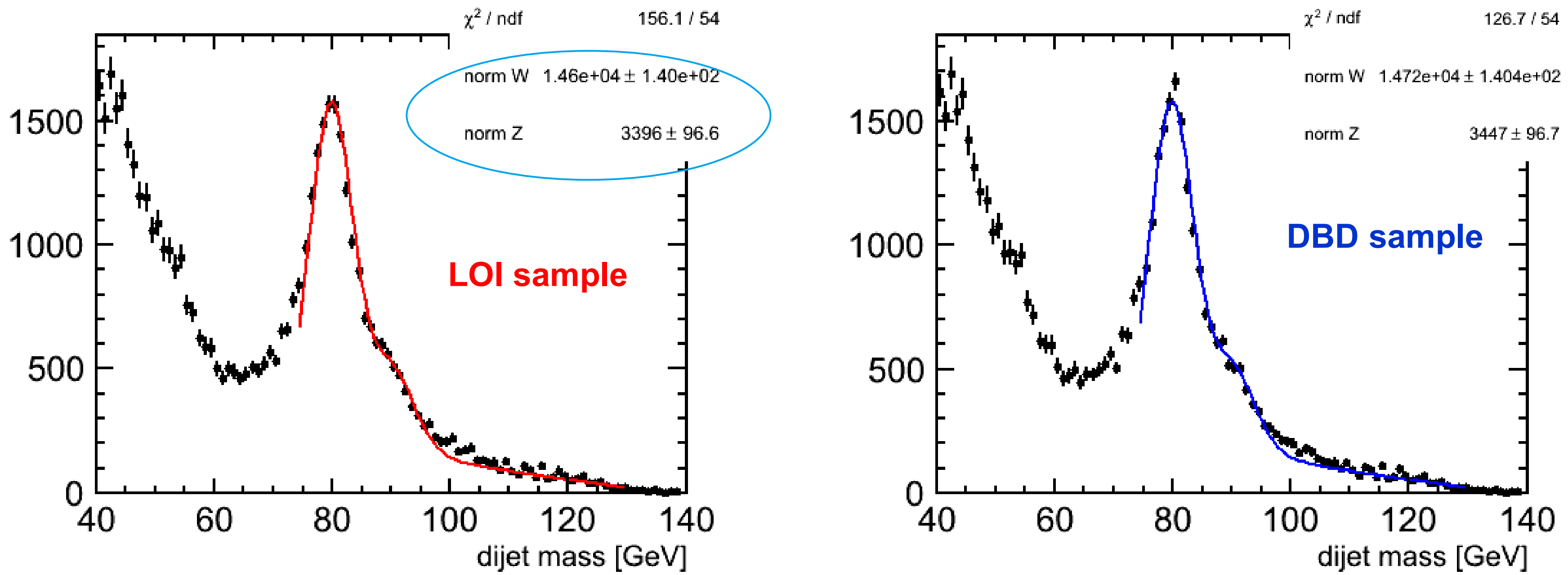

- σ ∽ norm W / Z → check the statistical error on norm W/Z
- **For both LOI and DBD samples, the statistical errors are almost identical**:
  - In the case of $\tilde{\chi}_1^\pm$: $\simeq 1$ %
  - In the case of $\tilde{\chi}_2^0$: $\simeq 2.8$ %
- The same precision is obtained for the LOI sample as in the LOI analysis.

$\tilde{\chi}_1^\pm$ and $\tilde{\chi}_2^0$ Mass Measurement

- Mass difference to LSP ($\tilde{\chi}_1^0$) is **larger** than M_Z
- Observe the decays of real gauge bosons
- 2 body decay → the edges of the energy spectrum are kinematically determined
- **Use dijet energy spectrum „end points“ in order to calculate masses**

$$\gamma = \frac{E_{beam}}{M_\chi}$$

$$E_\pm = \gamma \cdot EV^* \pm \gamma \cdot \beta \cdot \sqrt{E_V^{*2} - M_V^2}$$

Real [model] edge values [GeV]:

W_{low}	W_{high}	Z_{low}	Z_{high}
80.17	131.53	93.24	129.06

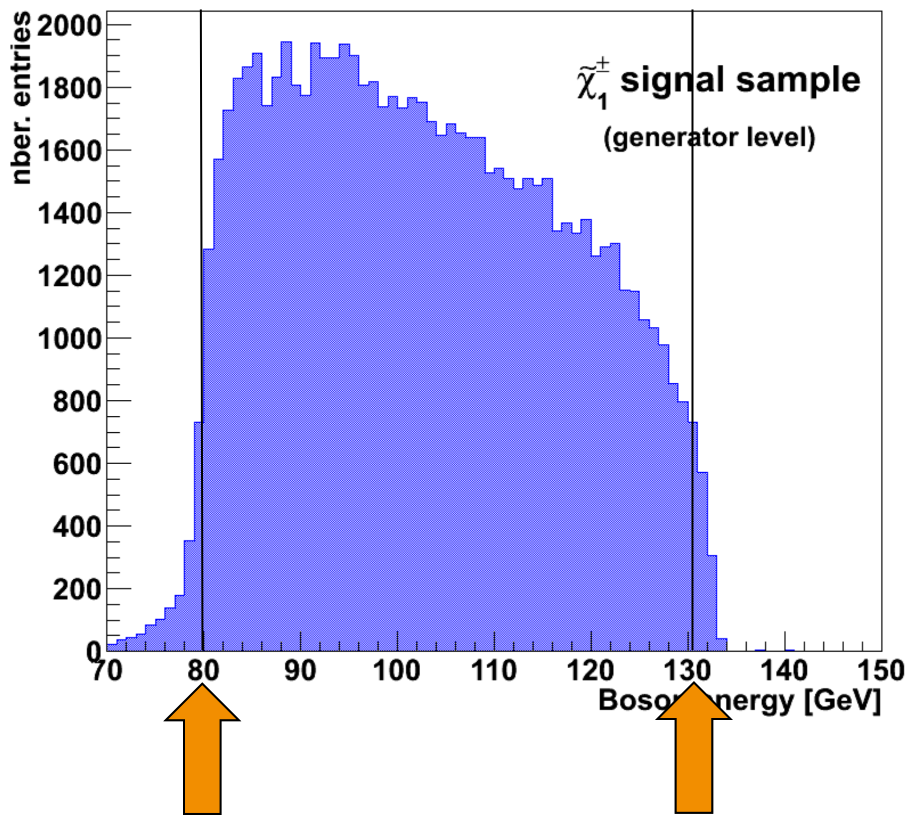

Dijet [Boson] Energy Comparison LOI - DBD

> **Use dijet energy to measure $\tilde{\chi}_1^{\pm}$ and $\tilde{\chi}_2^0$ mass**

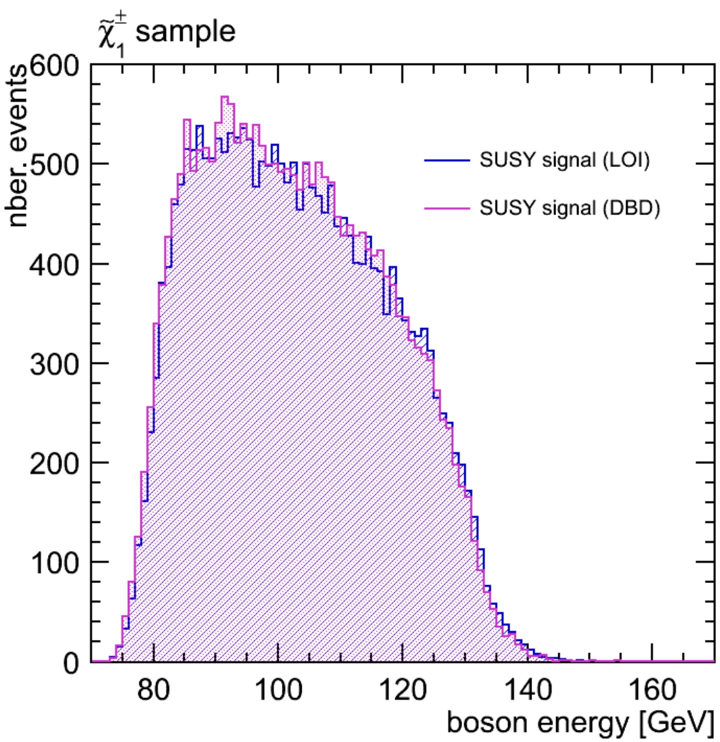

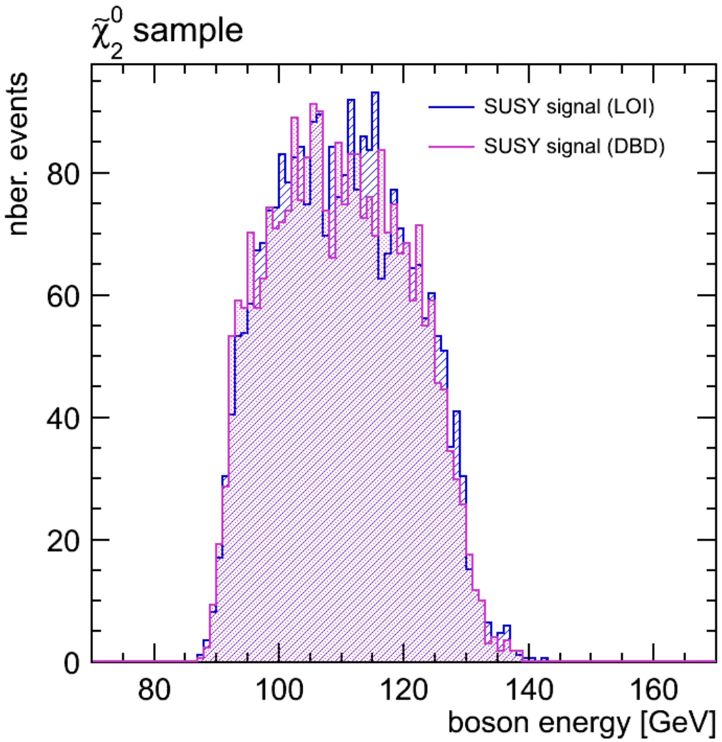

> The DBD distribution appears slightly shifted towards lower energies. Nevertheless, the two distributions agree very well.

$\tilde{\chi}_1^{\pm}$ and $\tilde{\chi}_2^0$ Signal Sample Further Separation

- Calculate χ^2 with respect to nominal W / Z mass

$$\chi^2(m_{j1}, m_{j2}) = \frac{(m_{j1} - m_V)^2 + (m_{j2} - m_V)^2}{\sigma^2}$$

$\Downarrow$

min $\chi^2 \rightarrow \tilde{\chi}_1^{\pm}$ and $\tilde{\chi}_2^0$ separation

- Downside: lose statistics
  - Cut away 43% of $\tilde{\chi}_1^{\pm}$ surviving events
  - Cut away 68% of $\tilde{\chi}_2^0$ surviving events
- However, after the χ^2 cut, the separation is quite clear:

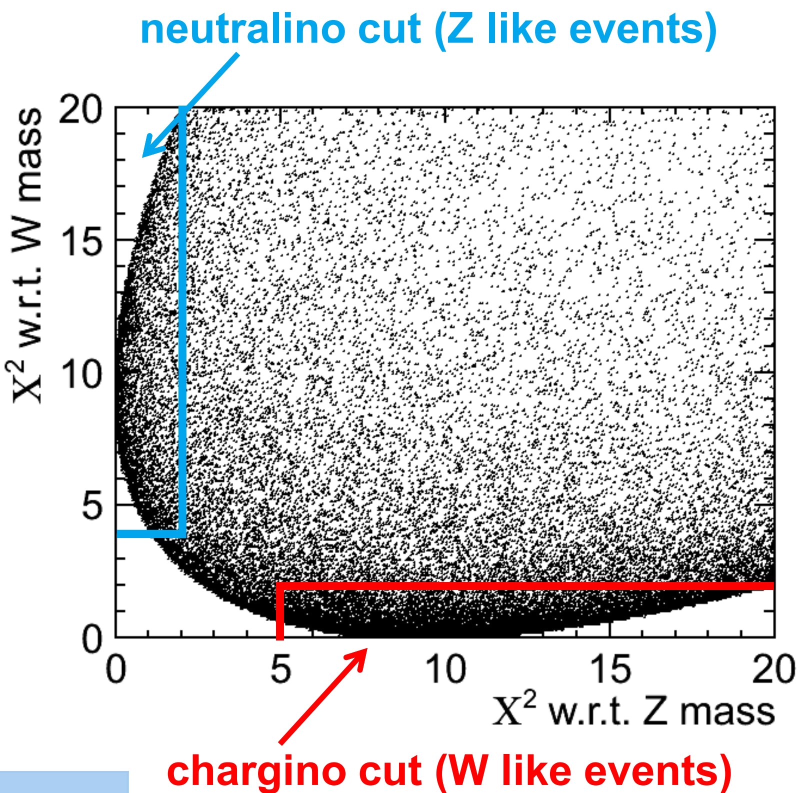

Obs.	DBD		LOI	
	$\tilde{\chi}_1^{\pm}$	$\tilde{\chi}_2^0$	$\tilde{\chi}_1^{\pm}$	$\tilde{\chi}_2^0$
Efficiency	57%	32%	56%	34%
Purity (total)	63%	35%	62%	35%
Purity (SUSY)	94%	68%	95%	66%

$\tilde{\chi}_1^\pm$ and $\tilde{\chi}_2^0$ Mass Measurement – "Endpoint" Method

> Fit dijet energy spectrum and obtain edge positions:

$$f(x; t_{0\_1}, b_{0\_2}, \sigma_{1\_2}, \gamma) = f S_M + \int_{t_0}^{t_1} (b_2 t^2 + b_1 t + b_0) V(x - t, \sigma(t), \gamma) dt$$

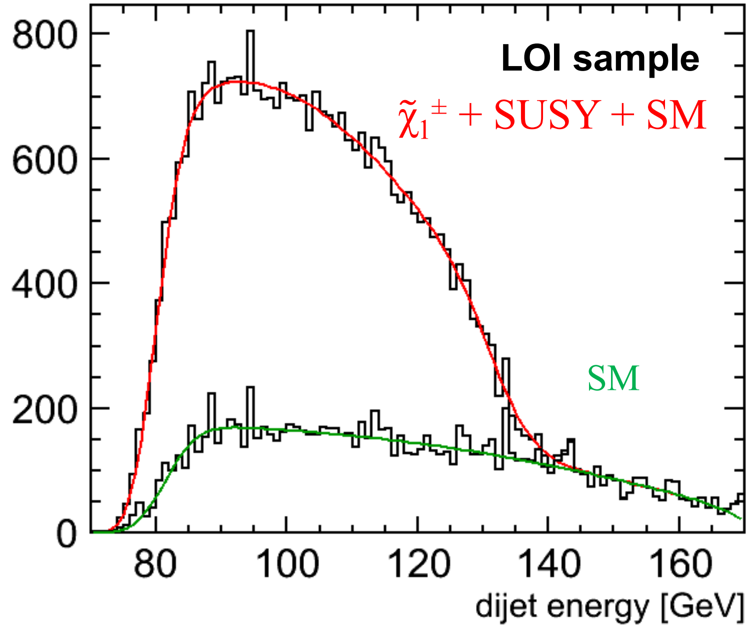

Where:

- The polynomial accounts for the slope of the initial spectrum
- The Voigt function accounts for the detector resolution and gauge boson width

Issues of the „Endpoint Method“

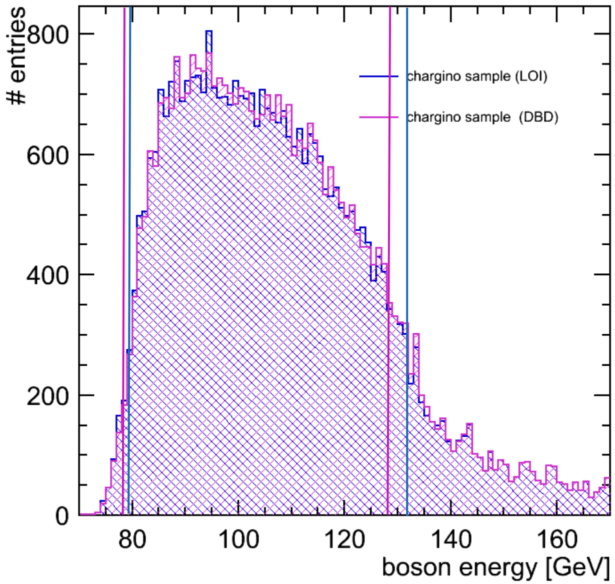

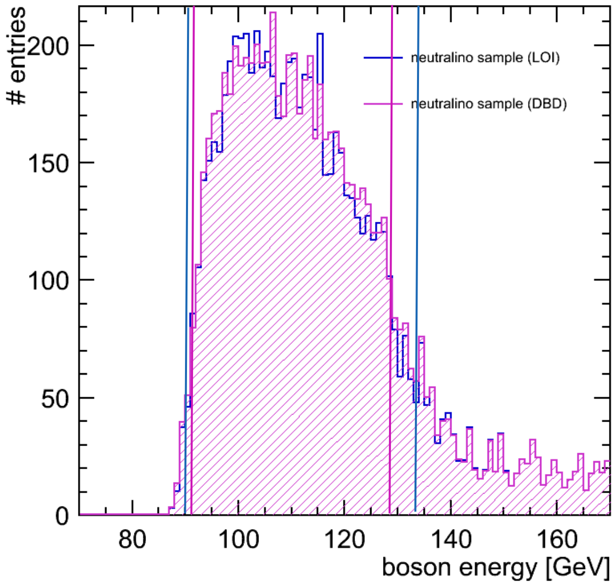

Sim.	Edge W_{low} [GeV]	Edge W_{high} [GeV]	Edge Z_{low} [GeV]	Edge Z_{high}[GeV]
DBD	79.5±1.7	128.3±1.2	91.9±0.8	127.9±0.7
LOI	79.7±0.3	131.9±0.9	91.0±0.7	133.6±0.5

The fitting method appears to be highly dependent on small changes in the fitted distribution → it is clearly NOT appropriate for a comparing the simulation and reconstruction performance.

We need to apply a different edge extraction method!

Endpoint Extraction using an FIR Filter

- Finite Impulse Response (FIR) filters are digital filters used in signal processing.
- FIR filters can operate both on discrete as well as continuous values.
- The concept of “finite impulse response“ ↔ **the filter output** is computed as a finite, weighted sum of a finite number of values from the filter input.

$$y[n] = \sum_{k=-M_1}^{M_2} b_k x[n-k]$$

$x[n-k]$: the input signal

b_k: the filter coefficients (weights)

- y is obtained by convolving the input signal with the (finite) weights
- FIR filters are used to detect edges in image processing techniques:

D. Demigny, T. Kamlé

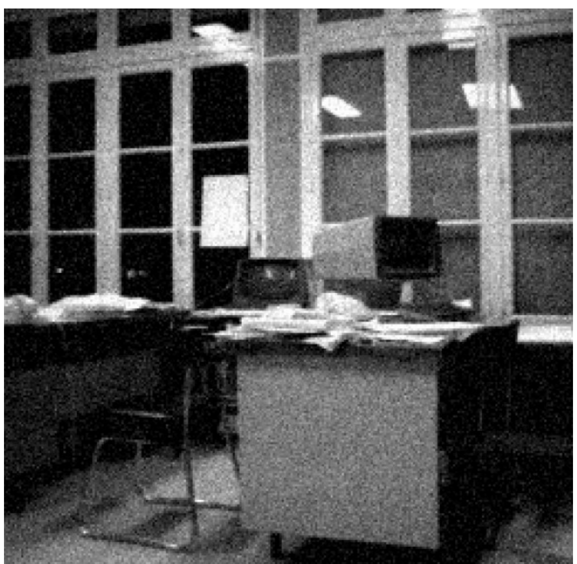

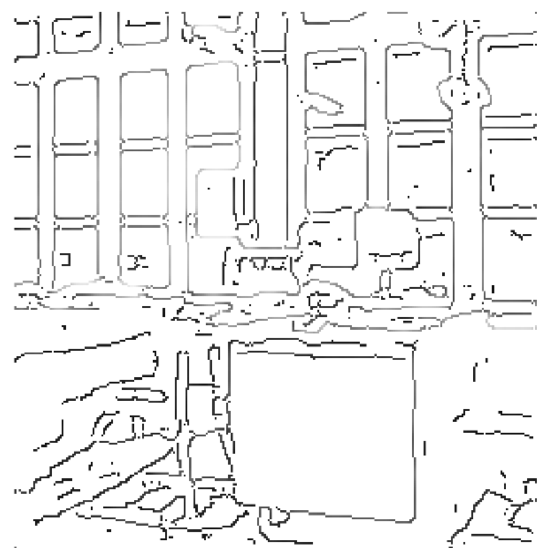

Testing the FDOG Filter

- J.F.Canny* has suggested that an optimal filter is very similar to the first derivative of a Gaussian
- There are two important filter characteristics that must be optimised:

the bin size

the filter size

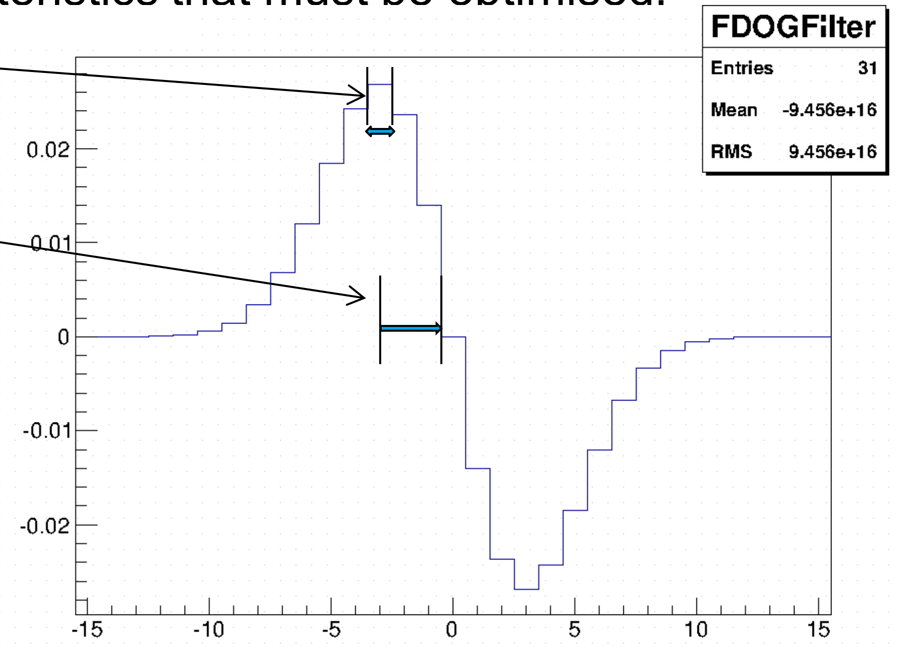

It is crucial to strike the right balance between the two:

- If the bin size is too small → the filter picks up a lot of statistical fluctuations
- If the filter size is too large → the edge position cannot be localised anymore

A toy MC study is needed to optimise the filter and bin size!

*) Canny's criteria: [J. F. Canny. **A computational approach to edge detection.** *IEEE Trans. Pattern Analysis and Machine Intelligence*, pages 679-698, 1986]

Testing the FDOG Filter

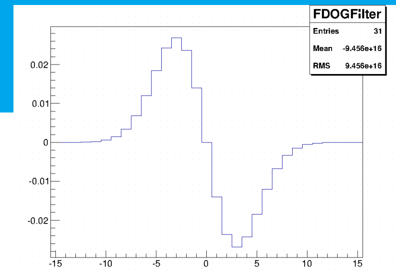

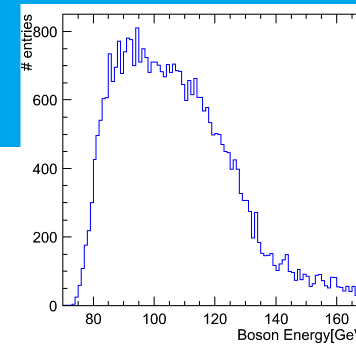

- There are two important filter characteristics that must be optimised: the bin size and the filter size.

Filter response after applying the FDOG Filter to the $\tilde{\chi}_1^{\pm}$ energy distribution:

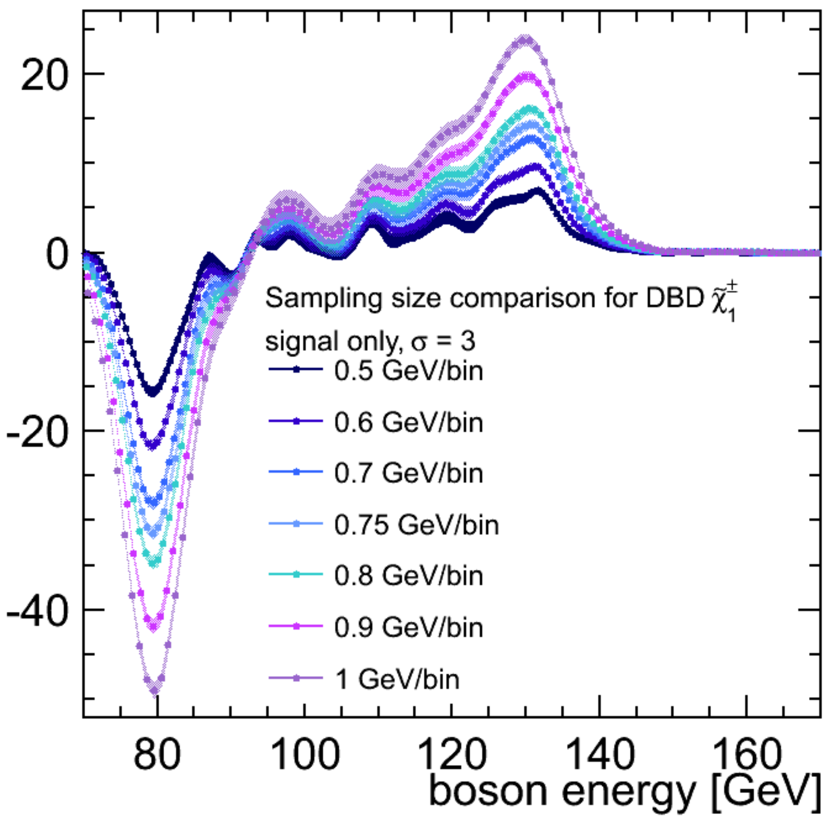

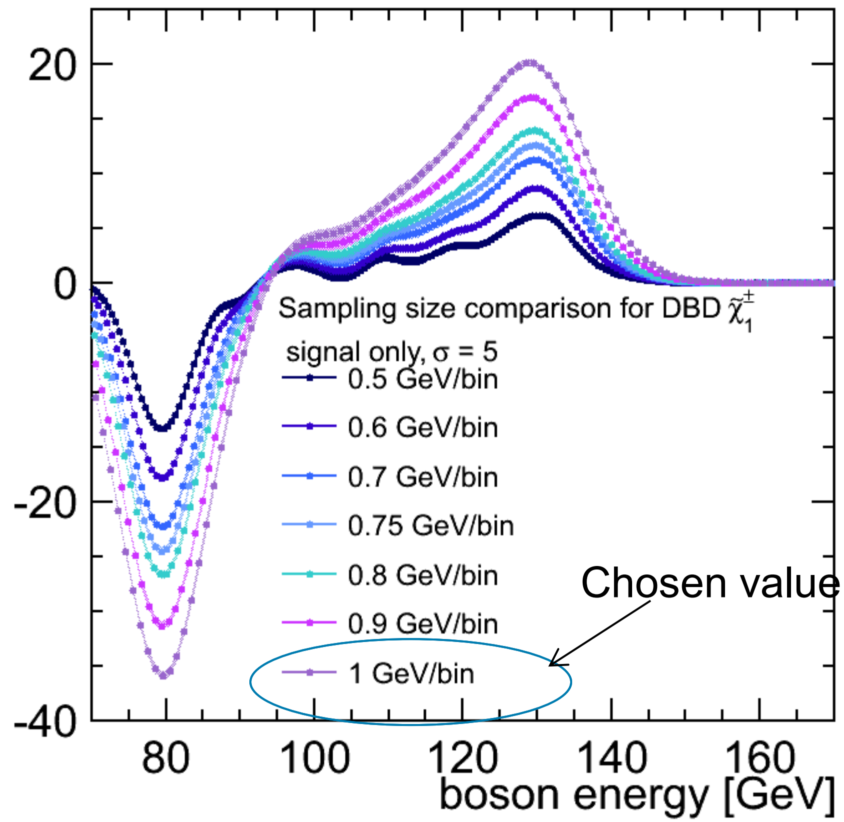

FIR Edge Extraction Comparison – LOI to DBD

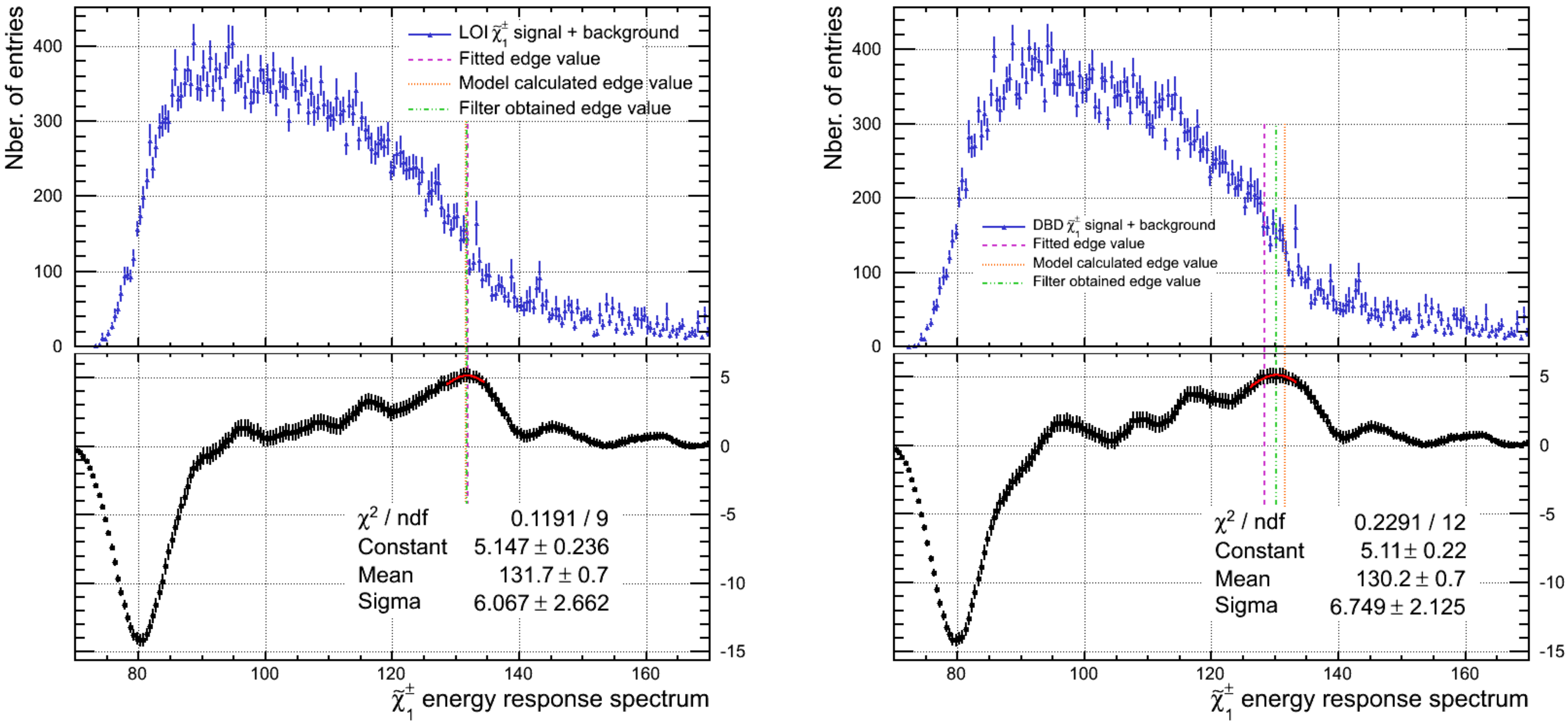

In the **LOI** case: the fitted and filter values are extremely close to the real model value.
In the **DBD** case: the filter value is much closer to the model one than the fitted edge.

Toy MC for the Filter Edge Extraction

- To estimate the statistical precision of the edge extraction → toy MC
- 10000 $\tilde{\chi}_1^{\pm}$ and $\tilde{\chi}_2^{0}$ energy spectra have been produced
- The FDOG filter was then applied 10000 times
- Example: for the $\tilde{\chi}_1^{\pm}$ case:

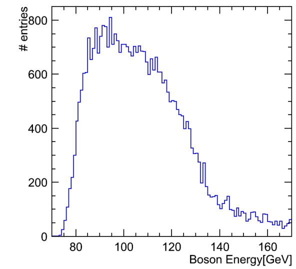

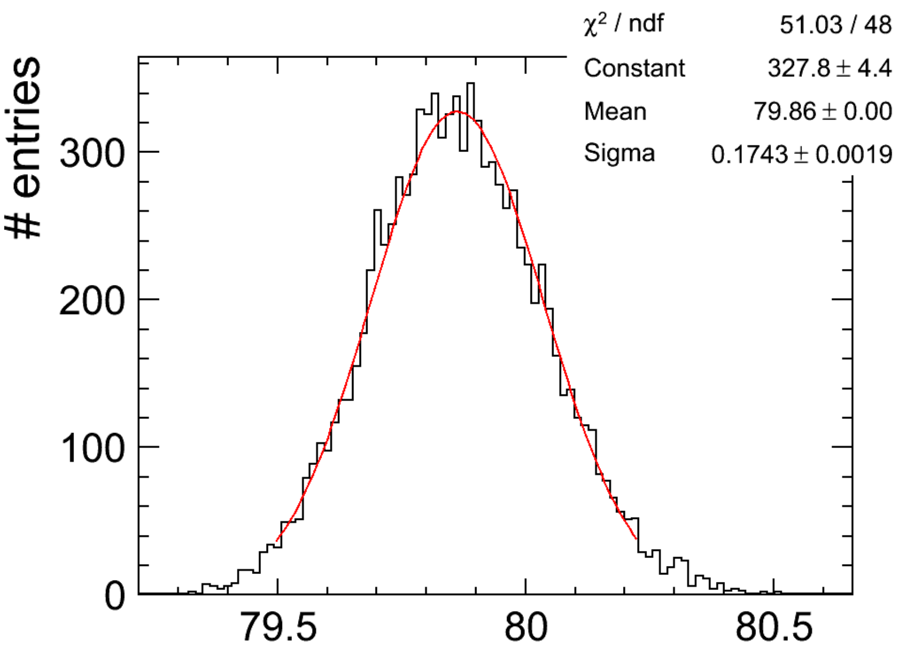

(low edge)

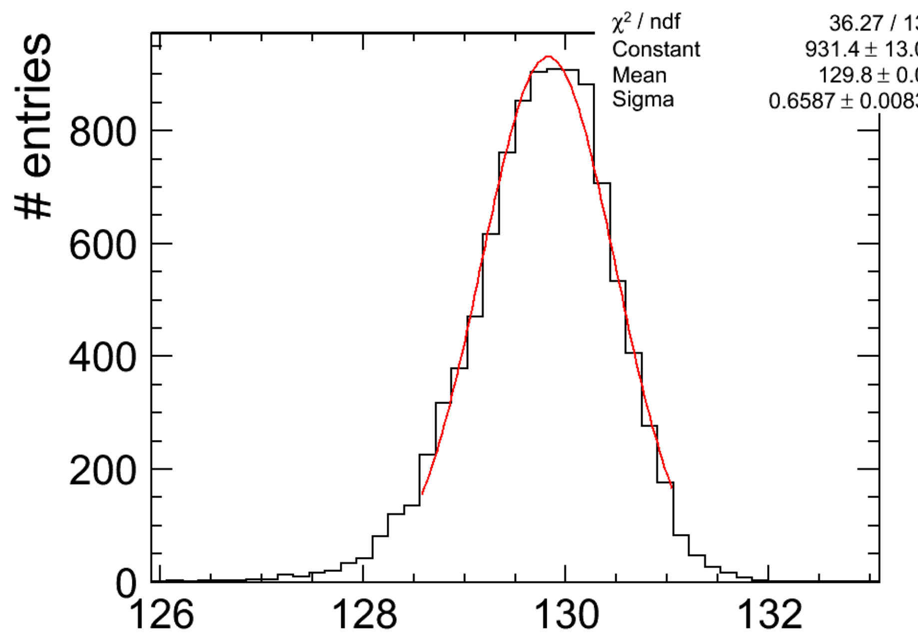

(high edge)

Edge Extraction Comparison

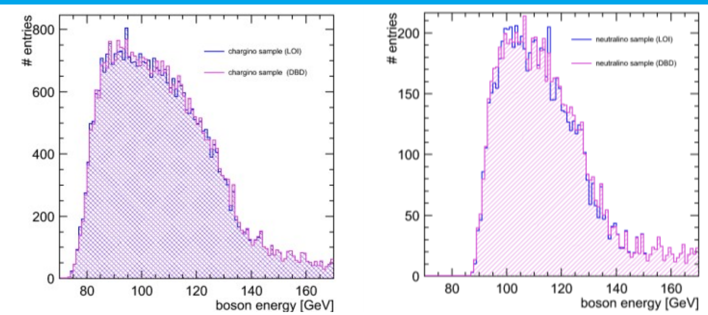

	Sim.	Edge W_{low} [GeV]	Edge W_{high} [GeV]	Edge Z_{low} [GeV]	Edge Z_{high}[GeV]
	True	80.17	131.53	93.24	129.06
	LOI	79.7±0.3	131.9±0.9	91.0±0.7	133.6±0.5
	DBD	79.5±1.7	128.3±1.2	91.9±0.8	127.9±0.7
filter	LOI	80.3±0.6	131.7±0.7	91.6±0.7	129.0±0.6
filter	DBD	80.1±0.2	130.2±0.7	91.9±0.2	127.2±0.7

- The LOI uncertainties do not change much.
- The filter results are comparable between LOI and DBD in central value.
- The lower edges are much more precise with the filter method.

The filter extraction method is preferable:

- it is more stable
- provides smaller uncertainties in determining the edge position.

Conclusions

- A preliminary comparison between the LOI and DBD simulation and reconstruction has been made;
  - The DBD reconstructed dijet masses and boson energies are compatible to the LOI analysis.
  - The fitting method for the mass determination appears very sensitive to small changes. A more robust method is needed.
  - Applying a finite impulse response (FIR) filter in order to extract the edge information instead of the fitting method is:
    - More robust (i.e. independent on distribution shape)
    - Provides just as good if not better statistical precision

> Outlook:

- Perform comparison on Full LOI and Full DBD data (update soon)
- Perform mass calibration (to determine systematics).
- Perform 2D fit on dijet masses to improve the x-section measurement

Thank You!

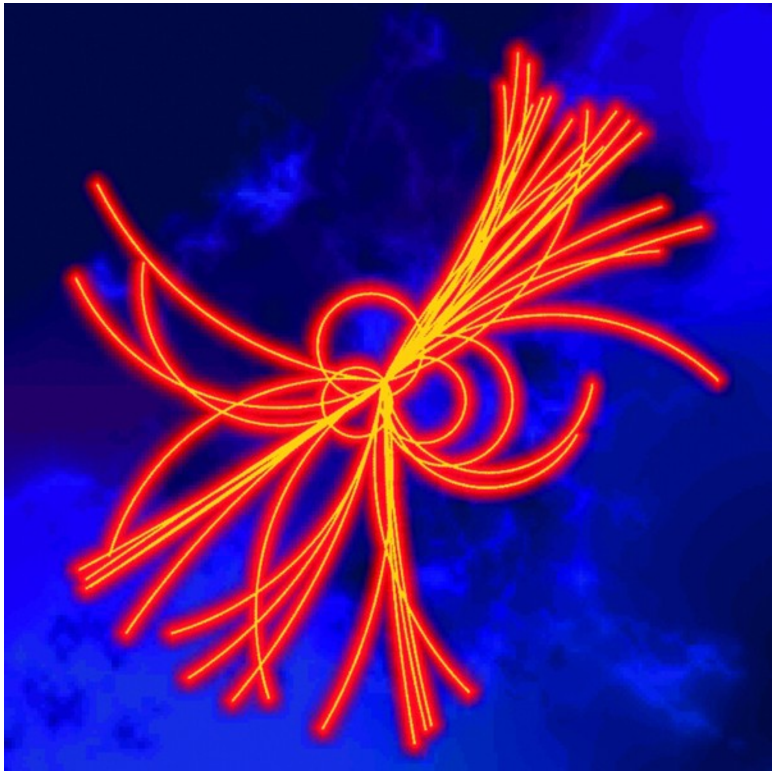

Back up slides

$\tilde{\chi}_1^{\pm}$ and $\tilde{\chi}_2^0$ Cross Section Measurement

> Separating W and Z pairs candidates:

- SM background fitted with polynomial
- Signal distributions fitted with Voigt profile
  - Width (Γ) set to boson's natural width (2.11 GeV for W and 2.5 GeV for Z
  - Voigt $\sigma \simeq 3.5$ GeV detector resolution, deduced from a SM sample. The σ from the signal only sample is in the same ballpark!
- Determine relative W/Z fractions from fit

Example: DBD sample

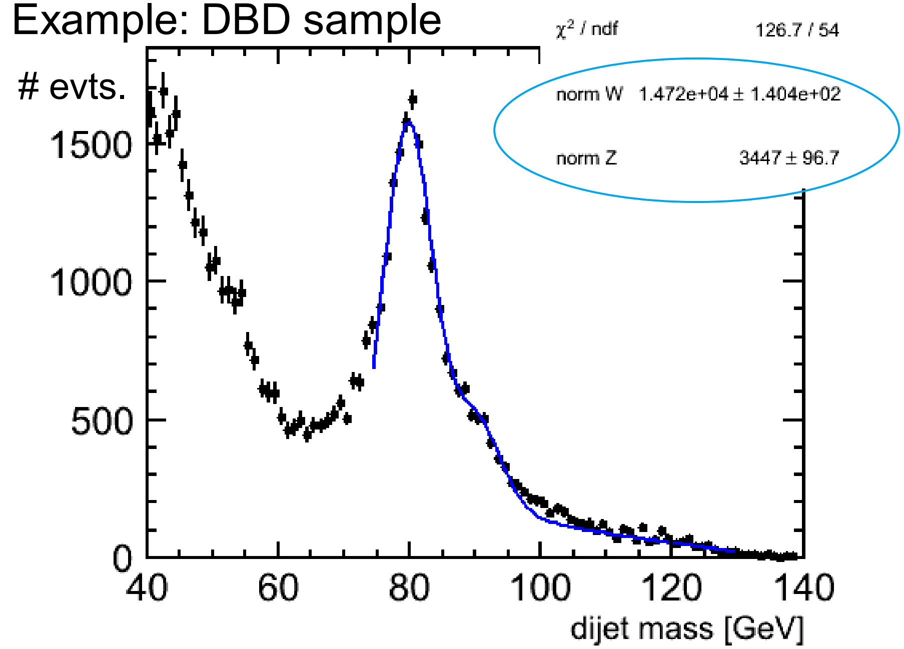

Endpoint Extraction Comparison – LOI to DBD

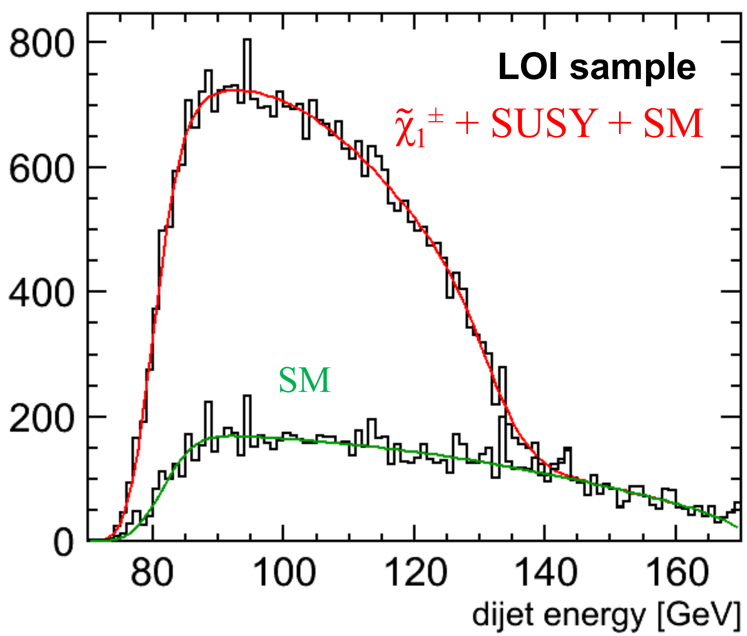

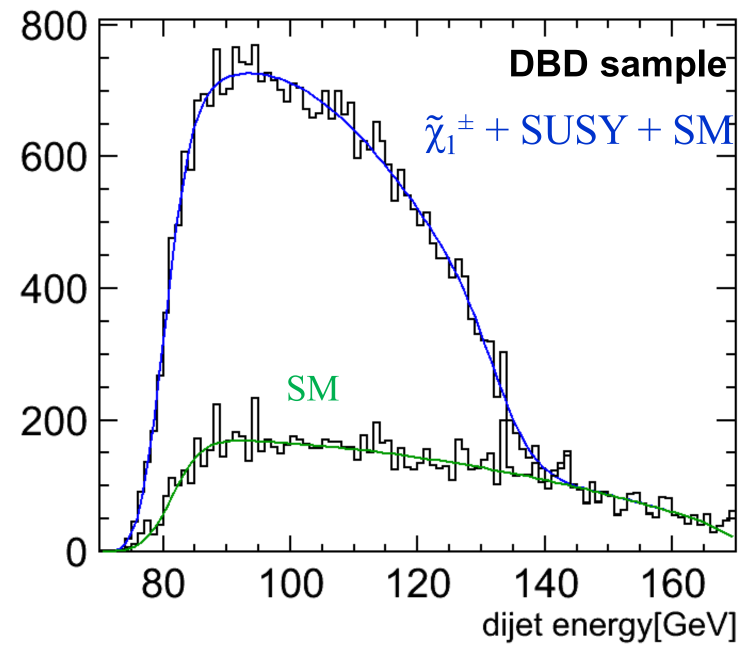

$E_{low} \simeq 79.7 \pm 0.3$ GeV
$E_{high} \simeq 131.9 \pm 0.9$ GeV

$E_{low} \simeq 79.5 \pm 1.7$ GeV
$E_{high} \simeq 128.3 \pm 1.2$ GeV

- The DBD distribution appears slightly shifted towards lower energies. Nevertheless, the two distributions agree very well.

Applying an FIR Filter – Example: the box function

> The changes of a function can be described by the derivative → interpret the histogram as a 1D function

> The points that lie on the edge of the distribution → detected by local maxima and minima of the first derivative

$$f'(x) = \lim_{h\to 0} \frac{f(x+h)-f(x)}{h} \approx f(x+1) - f(x) \quad (h=1)$$

> The first derivative is approximated by using the **kernel [-1, 0, 1]**

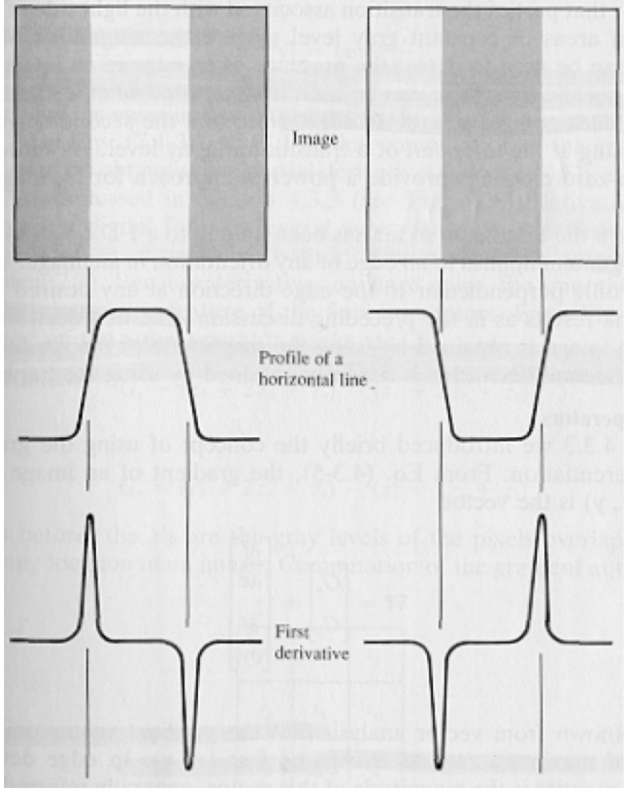

Applying an FIR Filter – Example: the box function

- The changes of a function can be described by the derivative → interpret the histogram as a 1D function
- The points that lie on the edge of the distribution → detected by local maxima and minima of the first derivative

$$f'(x) = \lim_{h \to 0} \frac{f(x+h) - f(x)}{h} \approx f(x+1) - f(x) \quad (h = 1)$$

- The first derivative is approximated by using the **kernel [-1, 0, 1]**
- The kernel is convoluted with the histogram:

$$response_i = -1 \times bin_{i-1} + 0 \times bin_i + 1 \times bin_{i+1}$$

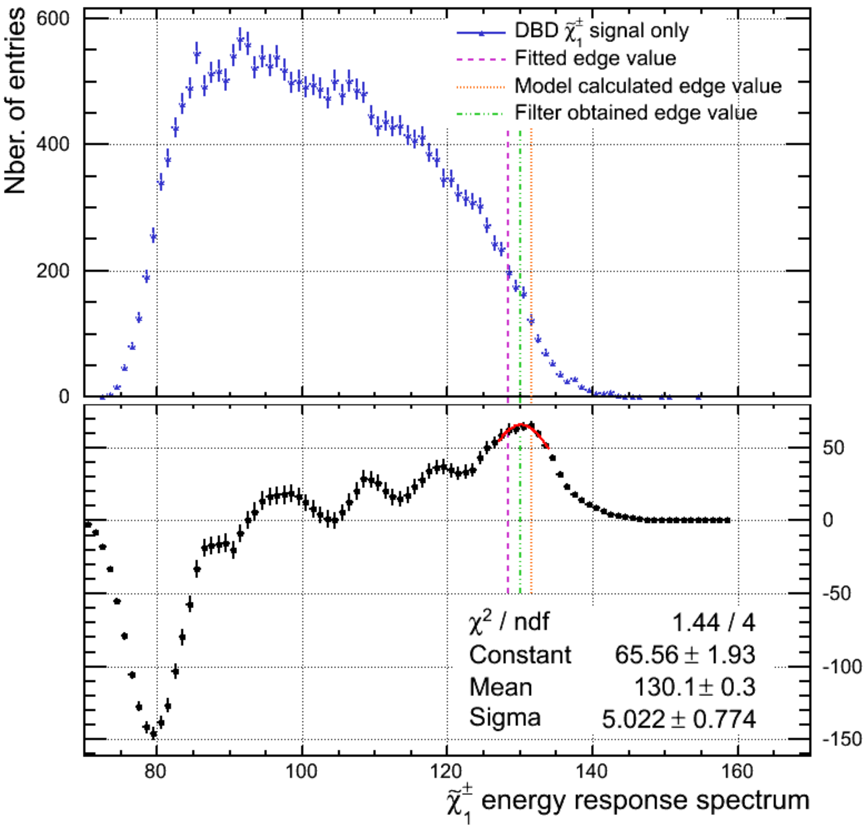

Applying an FIR Filter

- Goal: find edge positions in spectrum
- Strategy: use weighted sums of bin content values to find patterns in distribution

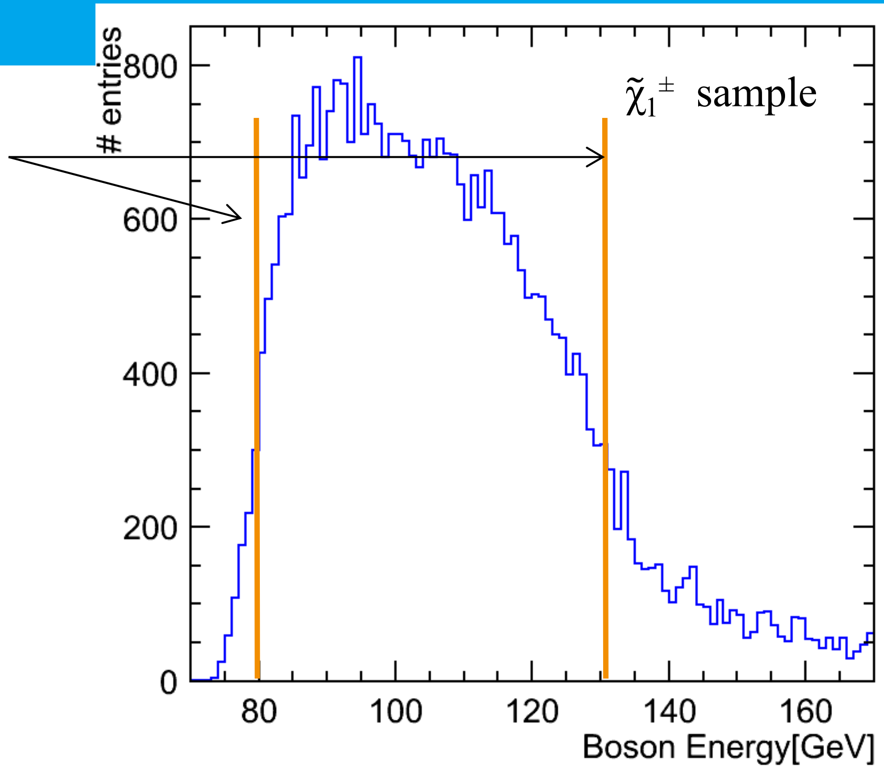

Applying an FIR Filter

- Goal: find edge positions in spectrum
- Strategy: use weighted sums of bin content values to find patterns in distribution
- Consider the histogram as an array of bin content values

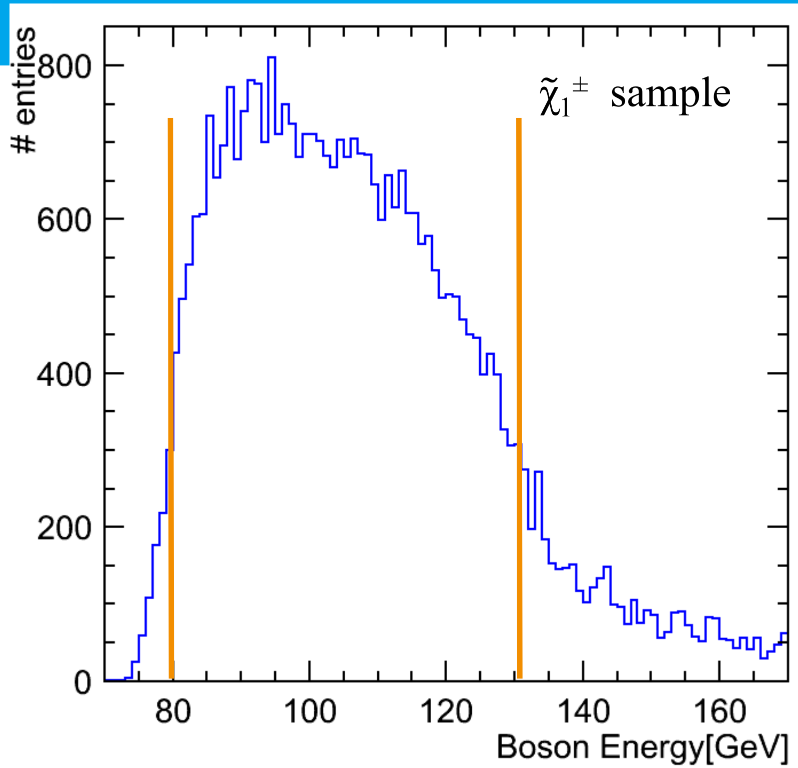

Bin #	1	2	3	...	98	99	100
Entries	0	15	28	...	34	22	4

Applying an FIR Filter

- Goal: find edge positions in spectrum
- Strategy: use weighted sums of bin content values to find patterns in distribution
- Consider the histogram as an array of bin content values
- Consider an array of chosen weights (smaller than the histogram!)
- Create new array of the same size:
  - Each entry in the new array is the weighted sum of the bin content values from the bins surrounding the corresponding bin in the original array.
  - The array is filled using the **same** (finite) weights each time.
- The value of the output depends on the pattern in the neighbourhood of the considered bin and NOT on the position of the bin
- The pattern of weights = kernel
- The filter application = convolution

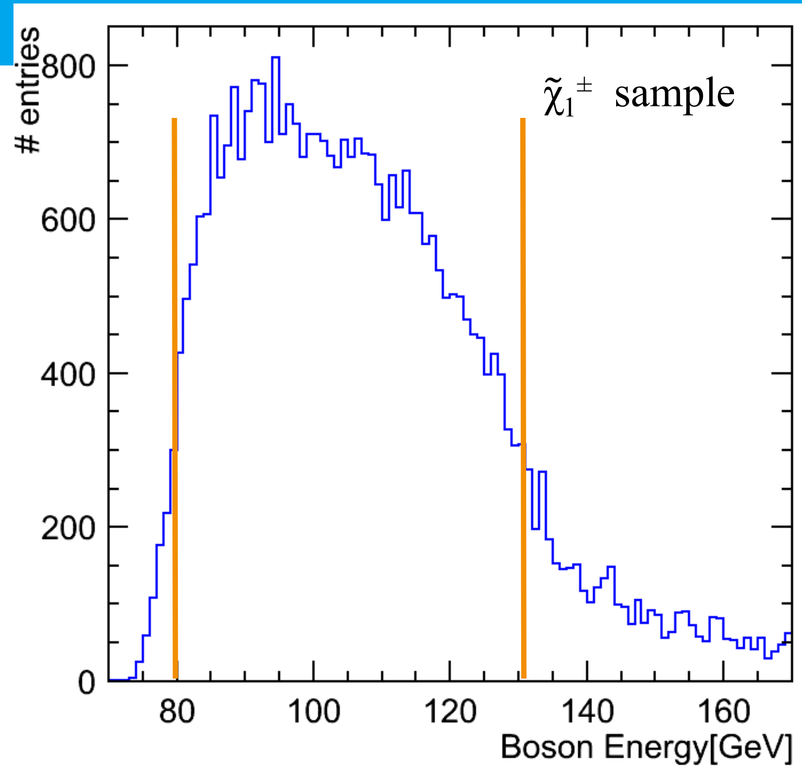

Bin #	1	2	3	...	98	99	100
Entries	0	15	28	...	34	22	4

$$w_1 \times 0 + w_2 \times 15 + w_3 \times 28 = \text{val2}$$

Entries	val1	val2	val3	...	val98	val99	val100

Testing the FDOG Filter

Studied the effect of the filter size on a smeared step edge monte carlo data.

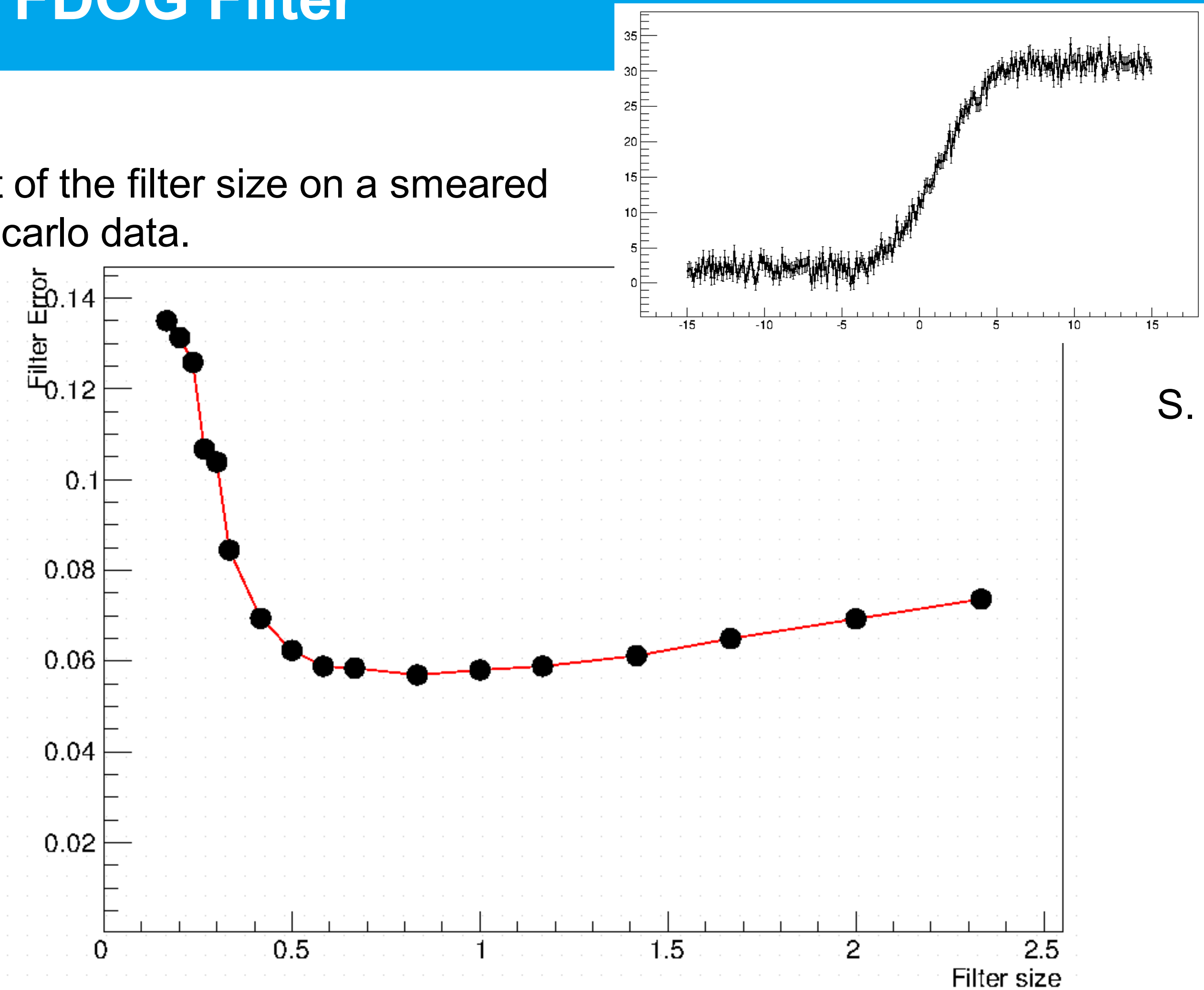

S. Caiazza

The FDOG filter does indeed perform best.
The filter size should be comparable to the size of the edge feature.
We chose $\sigma = 5$ bins.

Choosing the Appropriate Filter

- The first derivative as kernel works
- It is however a high pass filter → may be rather noisy
- In order to choose an apropriate filter one can apply the following criteria:

  Canny's criteria: [J. F. Canny. **A computational approach to edge detection.** *IEEE Trans. Pattern Analysis and Machine Intelligence*, pages 679-698, 1986]

  - Good detection: probability of obtaining a peak in the response must be high
  - Localisation: standard deviation of the peak position must be small
  - Multiple response minimisation: probability of false postive detection must be small
- Canny has suggested that an optimal filter is very similar to the first derivative of a Gaussian

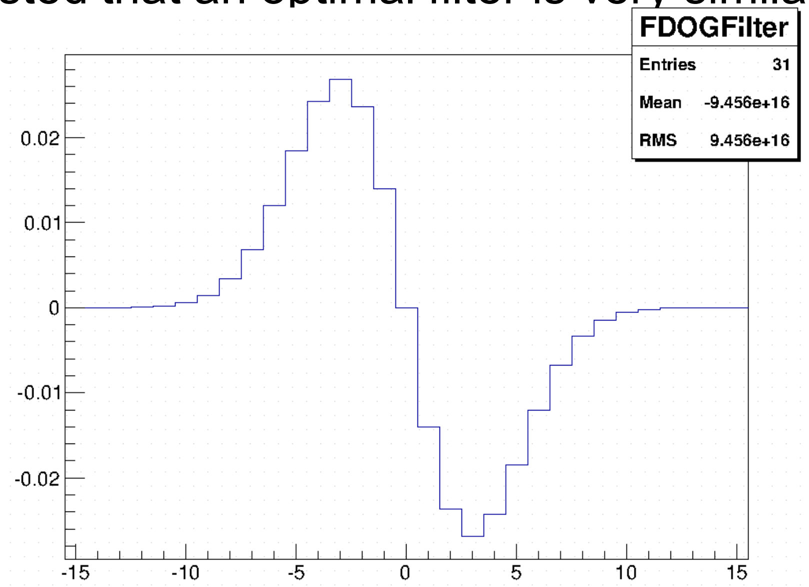

$\tilde{\chi}_1^{\pm}$ and $\tilde{\chi}_2^0$ Separation as Study case for Particle Flow

- Signal topolgy:
  4 jets and missing energy
- Event preselection (kinematics, etc.)
- Perform kinematic fit:
  equal mass constraint
  (determine best jet pairing)

Kinematic fit χ^2

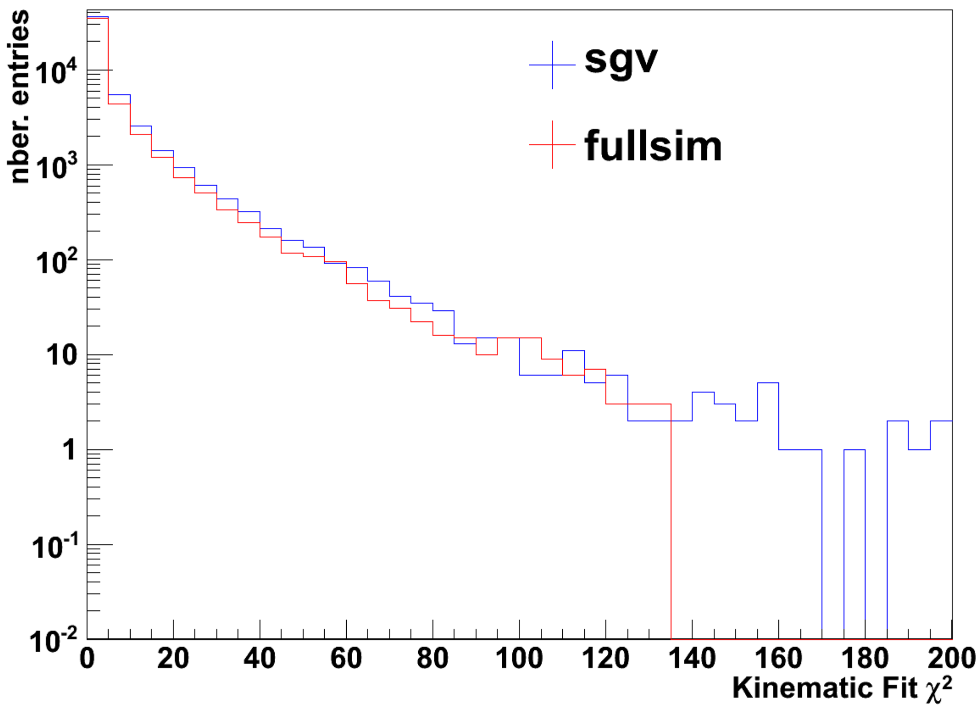

3.2. $\tilde{\chi}_1^{\pm}$ and $\tilde{\chi}_2^0$ Cross Section Measurement
3.2.2. 2D dijet mass fit

Distribution for SM + all signal

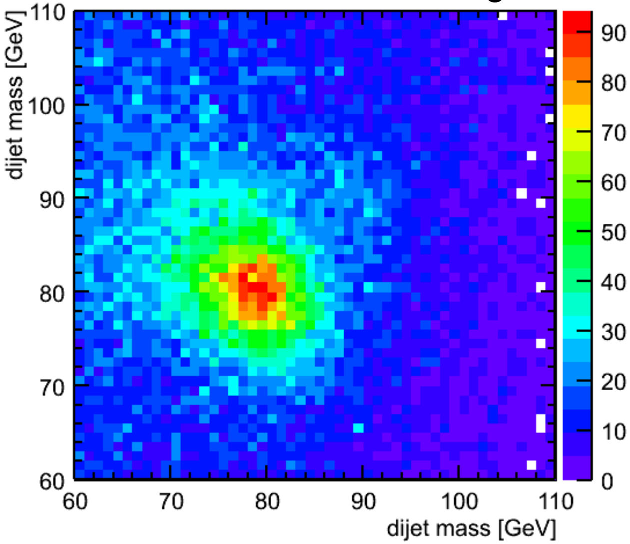

Example: DBD sample

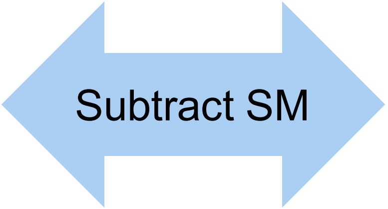

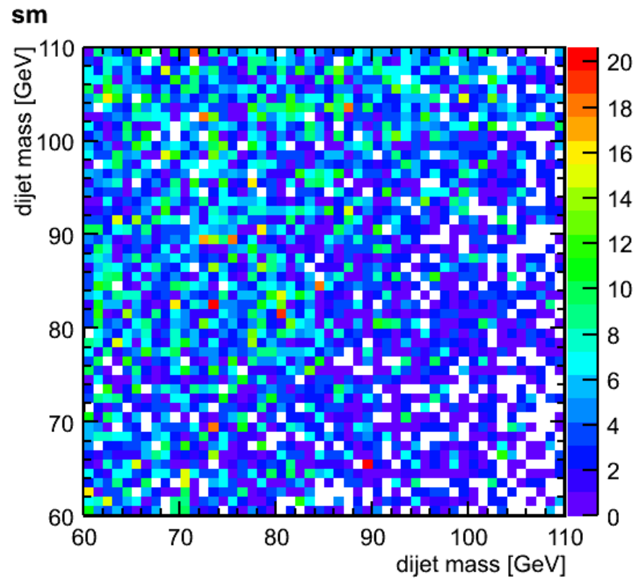

$\tilde{\chi}_1^{\pm}$ template that will be fit

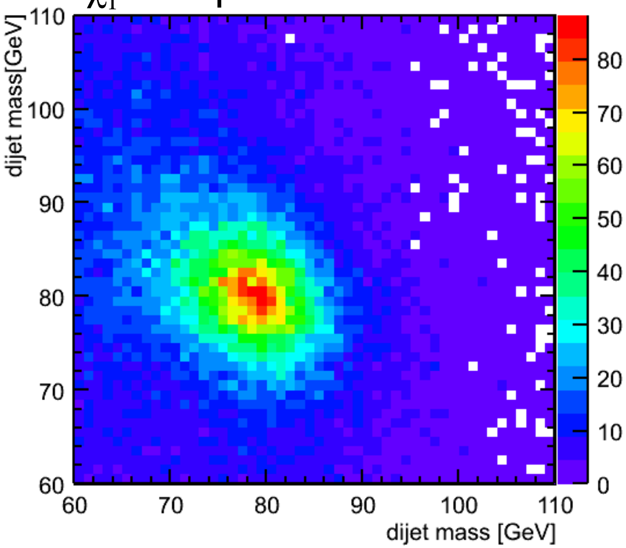

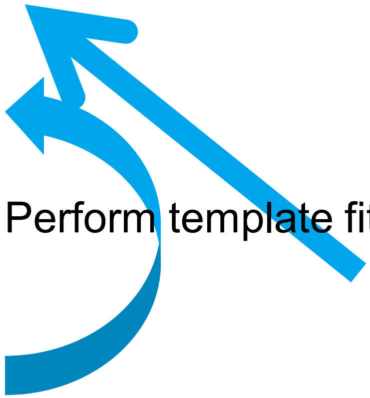

Perform template fit

$\tilde{\chi}_2^0$ template that will be fit